

Feasibility of Cardiovascular Magnetic Resonance of Angiographically Diagnosed Congenital Solitary Coronary Artery Fistulas in Adults

S. A. M. Said, MD,¹ M. B. M. Hofman, PhD,² A. M. Beek, MD,³ T. van der Werf, MD, PhD,⁴ and A. C. van Rossum, MD, PhD³

Department of Cardiology, Regional Hospital ZGT, Hengelo, The Netherlands¹

Department of Physics and Medical Technology, VU University Medical Centre, Amsterdam, The Netherlands²

Departments of Cardiology, VU University Medical Centre, Amsterdam, The Netherlands³

Radboud University Medical Centre Nijmegen, Nijmegen, The Netherlands⁴

ABSTRACT

Objective: To evaluate the use of cardiovascular magnetic resonance (CMR) to visualize angiographically-detected congenital coronary artery fistulas in adults. **Methods:** CMR techniques were used to study 13 patients, recruited from the Dutch Registry, with previously angiographically diagnosed fistulas. **Results:** Coronary fistulas were detected in 10 of 13 (77%) patients by CMR and, retrospectively, in two (92%) more. In 93% of these, it was possible to determine the origin and the outflow site of the fistulas. Cardiovascular magnetic resonance allowed demonstration of dilatation of the fistula-related coronary artery in all cases. Tortuosity of fistulas was detected in all visualized patients. Uni- or bilaterality of fistulas as seen on CAG was proven on CMR in all patients. Flow measurement could be performed in 8 patients. A fairly good correlation ($r = 0.72$) was found between angiographic (mean 6.2 mm, range 1–16) and cardiovascular magnetic resonance (mean 6.3 mm, range 3–15) measured fistulous diameters. **Conclusions:** Cardiovascular magnetic resonance of congenital fistulas with clinical significant shunting is feasible and can provide additional physiological data complementary to the findings of conventional coronary angiography.

INTRODUCTION

To date coronary arteriography (CAG) has been considered the “gold standard” for detection and delineation of the fistulous communications. There are several reports in the literature of noninvasive methods having been successfully used in the iden-

tification of such fistulas (1–6). A noninvasive technique such as cardiovascular magnetic resonance (CMR) may therefore become important as it provides excellent 3D imaging and accurate flow quantification (7). Flow quantification may give information on the amount of ventricular volume loading caused by a fistula, which may be relevant to the timing and method of treatment. CMR may, therefore, provide a supplement or substitute for coronary angiography, and the purpose of this report is to assess its value in visualizing angiographically proven congenital coronary artery fistulas (CAFs) in a series of adult patients. Current experience with CMR for the diagnosis of CAFs is limited to case histories (8–11). CAFs have varied consequences that range in importance from an incidental finding at CAG to important anomalies with hemodynamic significance and requiring intervention. CAFs can result in congestive heart failure due to sizeable left-to-right shunt, thromboembolic events, myocardial ischemia or infarction, infective endocarditis, ventricular and supraventricular arrhythmias or even sudden death secondary to rupture of an associated aneurysm of the fistula (1, 3, 5, 10, 12). For symptomatic patients, surgical or percutaneous permanent occlusion of the fistulas is widely accepted. However, controversies exist in the management of asymptomatic subjects

Received 4 April 2006; accepted 20 July 2006.

Keywords: Cardiovascular Magnetic Resonance, Congenital Coronary Anomaly, Coronary Artery Fistulas, Coronary Arteriography.

Presented in part at the Euro-CMR meeting, May 2005, Zurich.

The authors appreciate the assistance of Dutch Cardiac Centres (appendix 1) and of Mrs. M.A. Belderok and Mr. M. Mintjens during the preparation of the manuscript.

Correspondence to:

Salah A. M. Said, MD, FESC

Department of Cardiology

Regional Hospital ZGT

Geerdinksweg 141, 7555 DL Hengelo

The Netherlands

tel. + 31 74 2905 281; fax + 31 74 2905 289

e-mail: samsaid@home.nl

(5, 13, 14). We report the findings on CMR of morphological anatomy and flow quantification of 13 adult patients with previously known congenital CAFs. These patients were recruited from a national Dutch Registry, where both angiography and CMR were available (15).

MATERIALS AND METHODS

Patients

A group of 13 consecutive patients with CAFs, who gave their informed consent and were recruited from the Dutch Registry (DR) where both coronary angiograms and CMR were available, were investigated for the value of CMR in detecting the fistulas.

Data of the Dutch registry

The DR of congenital CAFs comprised 71 adults out of 30,829 patients who underwent coronary angiography. The data of the DR on CAFs have been described earlier in detail (15). In brief, between 1996 and 2003, a registry was started for collecting data of adult patients with CAFs. In the registry clinical data and coronary angiographic findings of 51 patients with congenital solitary CAFs and 20 subjects with coronary artery-left ventricle multiple micro-fistulas (16) were included.

Coronary angiography

Assessment of the size of the fistulous vessel was based on comparison with the angiography catheter diameter. For the definition of fistulous aneurysm, we adopted the definition of coronary aneurysm, which is angiographically defined as a coronary artery dilatation that exceeds the diameter of the normal adjacent segments or the diameter of the patient's largest coronary vessel by a factor of 1.5 (17). The pathway of the fistula was described by two terms: straight or tortuous and single or multiple. According to the outflow of the fistula, we defined the receiving vessel or cardiac chamber and singularity or multiplicity, respectively.

Cardiovascular magnetic resonance

We performed CMR using a 1.5 Tesla whole-body magnetic resonance scanner (Magnetom Sonata, Siemens, AERLNGEN, Germany). using a 4 element phased array radiofrequency receiver coil. First, black blood anatomical imaging was performed using a single shot turbo spin echo technique with half Fourier imaging, triggered to the heart rhythm in diastole (spatial resolution $1.7 \times 1.4 \times 5 \text{ mm}^3$). During a breath-hold, a series of 11 parallel axial or oblique slices were obtained. For more vessel detail, a recently developed coronary CMR technique was applied (18). This bright blood technique used a fat suppressed 3D steady state free precession pulse sequence (true FISP) applied during a breath-hold (spatial resolution $1.4 \times 1.3 \times 4 \text{ mm}^3$). A series of these thin slabs (2.4 cm) were placed to visualize the vessel anatomy in greater detail. In order to visualize entry jets of fistulas within other vascular structures cine imaging was applied. A standard true FISP cine sequence was acquired, as well as a breath-hold fast low-angle shot (FLASH) sequence

with improved sensitivity to flow dephasing effects (19). Areas where fistula entry points were detected on initial CMR images were re-imaged using appropriately located parallel cine views. Finally, the volume flow through the fistula was assessed through a plane perpendicular to the vessel. A phase sensitive flow quantification technique was applied within a breath-hold (spatial resolution $1.4 \times 1.2 \times 5.5 \text{ mm}^3$, temporal resolution 60 ms). Analyses of volume flow data was performed with the FLOW software package (Medis, Leiden, The Netherlands). Contours were manually drawn around the cross-section of the fistula on anatomic (magnitude) images, and the volume flow was calculated on the corresponding velocity map. By integrating all cardiac phases, the net volume flow was determined.

The evaluation of CMR was single blinded. The investigators (ACvR and AMB) knew that the patients had fistula but had no access to further details regarding origin, outflow, pathway and fistula-related arteries.

Statistical analysis

All continuous variables are presented as mean \pm standard deviation and discrete variables are expressed as frequencies and percentage. Linear correlations coefficients were assessed between the diameters calculated by CAG and measured by CMR. Nonparametric Bland-Altman analysis was performed for assessing agreement between two methods.

RESULTS

Patients

Patient baseline characteristics are displayed in Table 1. The mean age of the 13 patients was 57 years (range 30–79 years), of whom 4 were women and 9 were men.

Coronary angiographic examinations

A total of 14 CAFs were apparent in the 13 patients on angiography: one bilateral and 12 unilateral. The mean diameter of the 14 CAFs was 6.2 mm (range 1–16 mm). The fistulous communications originated from the proximal segment of the left anterior descending artery in 7 cases, left main stem once, right coronary artery (RCA) 4 times, and circumflex artery (Cx) twice. The outflow was into the pulmonary artery 6, right atrium 1, right ventricle (RV) 3, left atrium (LA) 1 and superior vena cava (SVC) 3 times.

Cardiovascular magnetic resonance

The evaluation of CMR was single blinded. On the first review, 11 of the 14 fistulas (79%) in 10 of the 13 (77%) patients were detected. On a second review, guided by angiographic information, 2 of the 3 initially undetected fistulas were retrospectively identified. Example of images obtained by CAG and CMR are shown in Figs. 1 and 2, demonstrating anatomical and physiological details (four consecutive images of Fig. 2, A–D demonstrate the details of the jet flow).

Table 1. Patient's characteristics and fistula detection

Case	Age and gender	Presenting symptoms	Management	Aneurysmal manifestation and detection		CAG	Fistula detection	Second revision
				Diameter (mm)	CMR			
1	52 M	ACP	CMM			pLAD → PA	No fistula detection	pLAD → PA
2	56 M	AP	CMM			pLAD → PA	pLAD → PA	
3	67 M	Arrhythmia	SL CABG MVP	57 × 57 saccular	45	Cx → CS-RA	Cx → CS-RA	
4	45 M	AP	CMM	6 × 9 fusiform	Missed	pLAD → PA	pLAD → PA	
5	60 F	AP, dyspnea and presyncope	CMM	28 × 33 saccular	25 × 24	RCA → SVC	RCA → SVC	
6	43 M	AP and palpitation	CMM			pLAD → PA	pLAD → PA	
7	56 F	ACP and palpitation	CMM	5 × 6 saccular	4 × 6	pLAD → PA	pLAD → PA	No fistula detection
8	30 F	Fatigue and dyspnea	CMM			pLAD → RV	No fistula detection	
9	71 M	ACP	CMM			pLAD → PA	pLAD → PA	
10	60 M	Arrhythmia	CMM			RCA → SVC	RCA → SVC	
11	79 M	AP	SL CABG			LMCA → SVC	LMCA → SVC	
12	66 M	AP	AVR CABG			RCA → RV	RCA → RV	
			CMM			CX → LA	CX → LA	
13	57 F	AP	CMM			RCA → RV	No fistula detection	RCA → RV

Abbreviations: CAG = coronary angiography, CMR = cardiovascular magnetic resonance, ACP = atypical chest pain, CMM = conservative medical management, pLAD = proximal left anterior descending coronary artery, PA = pulmonary artery, AP = angina pectoris, SL = surgical ligation, CABG = coronary artery bypass grafting, MVP = mitral valve plasty, Cx = circumflex coronary artery, CS = coronary sinus, RA = right atrium, RCA = right coronary artery, SVC = superior vena cava, RV = right ventricle, LMCA = left main coronary artery, AVR = aortic valve replacement, LA = left atrium.

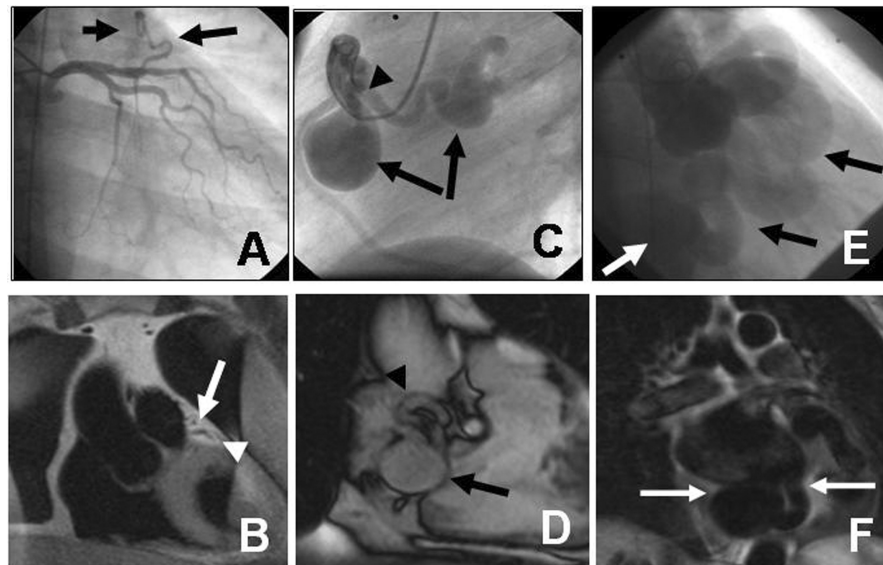


Figure 1. (A–F) Comparison of coronary angiographic and CMR images. A, (patient 4) The left coronary arteriogram in right-anterior oblique (RAO) projection demonstrating the fistula (long arrow) originating from the proximal LAD and outflow into the PA (short arrow). B, Trans-axial CMR cross section of the heart (spin echo technique) showing outflow of the LAD-fistula into the anterior side of the pulmonary artery (white arrow). A segment of the LAD is visible (white arrowhead). C, (patient 5): The right coronary arteriogram in left-anterior oblique (LAO) projection demonstrating the fistula (arrowhead) originating from the proximal RCA and its outflow into the SVC. Two aneurysms (arrows) are appreciated. D, CMR of the same patient showing the RCA in LAO equivalent view (coronal image) depicting the dilated fistulous vessel (white arrowhead) with one of the aneurysms (white arrow). The second aneurysm is outside the plane of the image. E, (patient 3) The aortogram in RAO projection demonstrating the fistula (black arrows) originating from the Cx and its outflow into the RA and coronary sinus (CS). Huge dilatation and ectatic fistulous vessel are noticeable. The CS shows aneurysmal dilatation (white arrowhead). F, CMR longitudinal view of the same patient demonstrating the dilated tortuous fistulous vessel (white arrows).

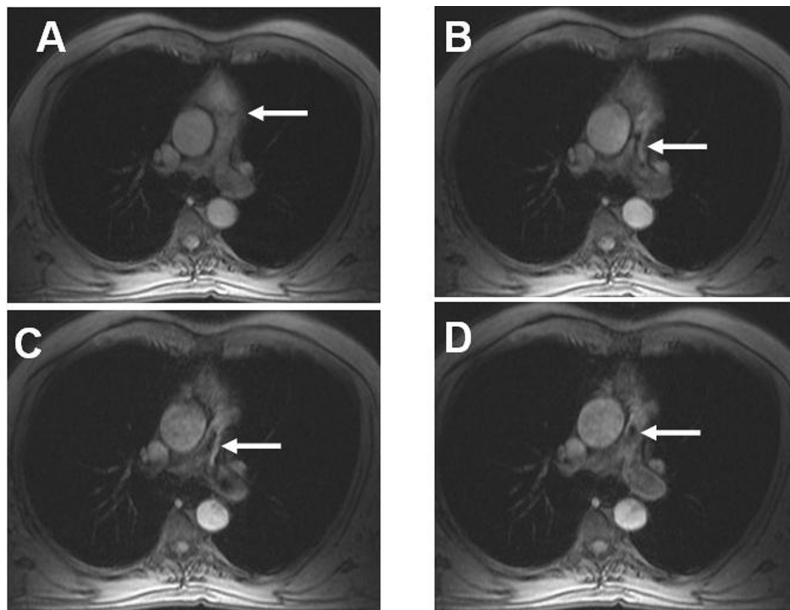
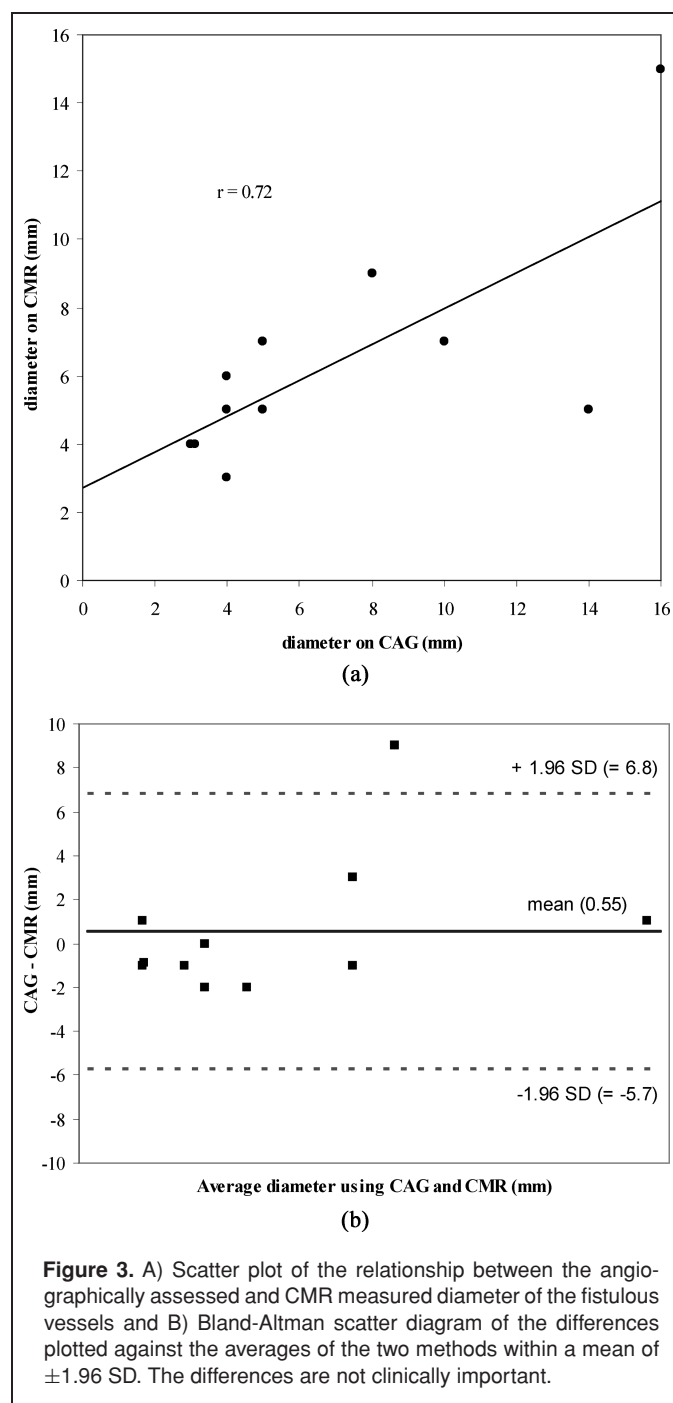


Figure 2. (A–D) Four consecutive CMR transverse T1-weighted slice images, from patient number 9, taken at 50, 150, 250 and 350 ms during diastole. The images were obtained with TE of 8.2 ms. Slice thickness of 7 mm. The arrows identifying the waxing and waning of a signal free space in the pulmonary artery during this part of the cardiac cycle. This phenomenon, called “flow void,” is caused by the outflow jet from the fistula into the pulmonary artery.

The mean diameter of the fistulous vessels was 6.3 mm (range 3–15 mm), providing good agreement ($r = 0.72$) with the diameter assessed by CAG. As demonstrated on Bland-Altman plots, there was no systematic trend found (20). Plot diagrams are shown in Fig. 3. Morphologic characteristics are listed in Table 2. Easy access of CAG relative to the limited availability of CMR resulted in delays between 1 and 112 months between the 2 investigations, with a median delay of 3 months.



Anatomical details (Table 2)

Origin

The origins of all 13 fistulas were identified in corresponding regions by CAG and CMR.

Outflow

In all fistulas, the outflow could be visualized by CMR and confirmed in cine images by signal loss at the site of the outflow jet. In one case (patient 11, of which outflow was to the SVC) the outflow was assessed by CMR as single while the CAG showed multiple outlets. The 3 other fistulas draining to the SVC were diagnosed correctly.

Pathway

In 3 fistulas, there were differences between the CAG and the CMR findings. In patient 5, the pathway was assessed on CMR to be multiple while on the CAG it proved to be single; this may be due to tortuosity of the fistulous vessel. In patient 10, the opposite was the case: on CMR, the pathway was diagnosed as single while it was seen on the CAG to be multiple. In patient 12 (first fistula, RCA \rightarrow RV), CMR could not provide a description of the pathway of one of the bilateral fistulas. It is striking that in all 3 of these disparities, the fistulas originating from the RCA.

Aneurysms

In 4 patients, 4 showed aneurysmal manifestation on CAG (patients 3, 4, 5 and 7). Three out of 4 aneurysms (1 fusiform and 2 saccular) were detected by CMR (Table 1). The missed aneurysm by CMR was of small diameter (6 \times 9 mm) (patient 4).

Failure of CMR in detecting CAFs (Table 3)

In the initial review, 3 fistulas were not detected. The angiographic diameters of these were 3, 1 and 10 mm, respectively. The fistulas originated from the proximal segment of the LAD in 2 patients (1 and 8) and from the RCA in one of the patients (patient 13). On the second CMR revision, 2 of the 3 fistulas were detected when guided by the angiographic road-map. The diameter of the undetected CAF was 1 mm, its course was straight, and no shunt was detected by CMR.

Failure of CMR to detect CAFs can be attributed to the small diameter of the fistulous vessel or inadvertent misidentification of the fistulous vessel as a normal branch because of localization of the fistula adjacent to the pericardium.

Physiology

Flow quantification could be performed in 8 out of 13 CAF patients. The average flow velocity measured in the fistulous vessel was 10 cm/s (range from 1.2–36). The mean flow quantification through the fistulas was 0.55 l/min (range 0.02–3.8). Individual results of all 13 patients are given in Table 4. In 5

Table 2. Anatomy of CAFs: Comparison between CAG and CMR findings

	CAG and diameter of fistulous vessel in (mm)				CMR and diameter of fistulous vessel in (mm)			
	Origin	Outflow	PW	Characteristics	Origin	Outflow	PW	Characteristics
1	pLAD Multiple	PA Single	Tortuous Multiple	Unilateral (3)	pLAD Single	PA At left anterior side Single	Tortuous Single	Overlooked on 1st occasion Revision: Technique of detection * 3-D FISP
2	pLAD Single	PA Single	Tortuous Single	Unilateral (4)	pLAD Single	PA 1.5 cm above PV at left anterior side Single	Tortuous Single	Unilateral (NA) Unilateral (5)
3	Cx Single	CS-RA Single	Tortuous Single	Unilateral (16) Aneurysm CAF Dilatation FRA	Cx Single	CS-RA Single	Tortuous Single	Unilateral (15) Dilatation of RA, LA, FRA and CS Aneurysm CAF
4	pLAD Single	PA Single	Tortuous Single	Unilateral (5) Aneurysm CAF	pLAD Single	PA 1.2 cm above PV at anterior side Single	Tortuous Single	Unilateral (5) No aneurysm detected
5	RCA Single	SVC Single	Tortuous Single	Unilateral (14) Aneurysm CAF Dilatation FRA	RCA Single	SVC Single	Tortuous Multiple	Unilateral (5) Aneurysm CAF Dilatation FRA
6	pLAD Single	PA Single	Tortuous Single	Unilateral (5)	pLAD Single	PA 1.7 cm above PV Single	Tortuous Single	Unilateral (7)
7	pLAD Single	PA Single	Tortuous Single	Unilateral (4) Aneurysm CAF	pLAD Single	PA Just above PV at left anterior lateral side Single	Tortuous Single	Unilateral (3) No aneurysm detected
8	pLAD Single	RV Single	Straight Single	Unilateral (1)	—	—	—	No fistula detection
9	pLAD Single	PA Single	Tortuous Single	Unilateral (3)	pLAD Single	PA 2.5 cm above PV Single	Tortuous Single	Unilateral (4)
10	RCA Single	SVC Multiple	Tortuous Multiple	Unilateral (4)	RCA Single	SVC Single	Tortuous Single	Unilateral (6)
11	LMCA Single	SVC Multiple	Tortuous Multiple	Unilateral (8)	LMCA Single	SVC 2 cm cranial to RAA Single	Tortuous Multiple	Unilateral (9)
12	RCA Single Cx Multiple	RV Single LA Multiple	Tortuous Single Tortuous Multiple	Bilateral (3)(7)	RCA Single Cx Multiple	RV Single LA Multiple	Not visible Not visible Tortuous Multiple	Bilateral (4) (NA) Dilatation of LA, LAA and LV
13	RCA Single	RV Single	Tortuous Single	Unilateral (10) Dilatation FRA	RCA Single	Junction area IVC and RA and distal CS Single	Unknown	Missed on 1st occasion Revision: Technique of detection * Unknown Unilateral (7) Dilatation of CS and FRA

Abbreviations: CAG = coronary angiography, CMR = cardiovascular magnetic resonance, PW = pathway, pLAD = proximal left anterior descending coronary artery, PA = pulmonary artery, FISP = fast imaging with steady-state precession, PV = pulmonary valve, Cx = circumflex coronary artery, CS = coronary sinus, RA = right atrium, CAF = coronary artery fistula, FRA = fistula-related artery, LA = left atrium, RCA = right coronary artery, SVC = superior vena cava, RV = right ventricle, LMCA = left main coronary artery, RAA = right atrial appendage, LAA = left atrial appendage, LV = left ventricle, IVC = inferior vena cava, NA = not available.

Table 3. Morphologic characteristics of missed CAFs by CMR

Patient	Fistula diameter	Origin	Outflow	Fistula characteristics	Sequence of detection
1	3 mm	LAD	PA	Origin: multiple, Outflow: single, PW: multiple/tortuous	Detected on second review
8	1 mm	LAD	RV	Origin: single, Outflow: single, PW: single/straight	Missed on both occasions
13	10 mm	RCA	RV	Origin: single, Outflow: single, PW: single/tortuous	Detected on second review

Abbreviations: CMR = cardiovascular magnetic resonance, LAD = left anterior descending coronary artery, PA = pulmonary artery, RCA = right coronary artery, RV = right ventricle, PW = pathway.

other fistulas, the flow measurements could not be analyzed due to poor image quality caused by improper breath-holding.

Diastolic flow exceeded systolic flow in most cases. In mid-systole there was a dip followed by an increase towards the end of systole. In diastole flow generally increased gradually until end-diastole; in patients 3 and 10, there is a discrete mid-diastolic peak. In the 3 patients (patients 3, 11 and 12) with the largest fistulas associated with the highest flow through the fistula, surgical ligation in combination with coronary artery bypass grafting was performed. Among the Dutch Registry patients evaluated, there was no uniform oxymetrically calculated left-to-right shunt volumes available because it was based on retrospective registry data and a prospective protocol was lacking.

DISCUSSION

The present study is one of the first to investigate the feasibility of CMR for the detection of congenital coronary artery fistulas in adult patients. It demonstrated that CMR could initially identify fistulas in 79% of the cases. A second review under angiographic imaging guidance identified 92% of the angiographically established fistulas.

Until now CAG has been considered the standard for visualization of CAFs, but the relation of CAFs to other structures, their origin, and course may not always be apparent by this method. CMR may be of value for complementary imaging with diagnostic anatomical and physiological work-up, and eventually for follow-up (1).

Previously published papers concerning CMR and CAFs were mainly based on case reports (1-6), which included individuals who were, on average, younger, more often symptomatic, and with considerably more comorbidities requiring surgical or nonsurgical interventional procedures (21) than found in our current series. Several authors recommend the use of CMR as a diagnostic tool for pre-interventional work-up of CAFs (4, 8, 9, 22).

Our study shows that CMR is capable of detection of 92% of the fistulas. Smaller fistulas and small aneurysms were missed by CMR, but these are without clinical consequence. In some patients, measurement of the shunt flow may give pivotal information which may influence the clinical decision making. The findings of high flow through the shunt in patients 3, 11 and 12 did not alter but enforce the clinical management.

Failure to identify this fistula by CMR is likely due to the lack of spatial resolution, compared to angiography, though a learning curve effect cannot be excluded. Detailed characteristics of the missed fistulas are shown in Table 3.

CMR was capable of identifying tortuosity in 79%, multiplicity of pathways in 57% and multiplicity of the origin in 93% (Table 5). Furthermore, CMR determined the distance of origin of the CAFs with regard to the left main stem and outflow into the cardiac structures, diameter of the fistula-related artery, diameter of the fistulous vessel and assessment of dimension of the cardiac chambers (Table 2).

Current MR sequences have improved image quality with superior anatomical definition, pointing to CMR as an alternative diagnostic tool for evaluating anatomy, physiology and function (4, 10-12). Recent advances in fast CMR have facilitated

Table 4. Characteristics, diameters and flow data of the fistulous vessels

Case	Diameter (mm)		Flow data	
	CAG	CMR	Velocity (cm/sec)	Volume (mL/min)
1	3	—	—	—
2	4	5	2.9	30
3	16	15	36	3835
4	5	5	9.4	85
5	14	5	—	—
6	5	7	2.4-3.6	—
7	4	3	—	—
8	1	—	—	—
9	3	4	2.4	20
10	4	6	1.2	15
11	8	9	14.4	550
12	3	4	18	130
	7	—	—	—
13	10	7	—	—

Table 5. CMR results of the different components of the fistula

	Number of fistulas (%)
Detection	
First review result	11/14 (79%)
Second review result	13/14 (93%)
Origin	
Donating vessel	13/14 (93%)
Single/multiple	13/14 (93%)
Pathway	
Straight/tortuous	11/14 (79%)
Single/multiple	8/14 (57%)
Outflow	
Site	12/14 (86%)
Single/multiple	11/14 (79%)
Aneurysms	3/4 (75%)

its clinical use for imaging blood flow through the coronary arteries (23) and could enhance the detection rate of CAFs as breath holding was a major determining factor in the fistulous flow assessment by CMR. Another advantage of CMR is its noninvasiveness.

The ability of conventional CMR to detect CAFs may, however, be limited when the shunt is small and the donor artery is not dilated (9). This is particularly true when fistulas drain into the right side of the heart such as right ventricle (2×) or pulmonary artery (1×), as was the case in the three unidentified fistulas in this study.

Few discrepancies were found between the CAG and CMR assessed fistula morphological description (Tables 2 and 4). These discrepancies can be explained by the lack of accuracy in CAG assessed diameters of the fistulous vessels. Secondly, a discrepancy might be due to the differences in CMR sequence methods.

CMR visualization of coronary fistulas is not easy, and a final analysis of images is time consuming, making the technique unsuitable for initial screening. It may, however, be of great value for complementary imaging and diagnostic work-up as the shunt measurement is reliably performed by CMR.

Suggested criteria for fistula detection by CMR

On the basis of previous findings (8, 10-12) and our own experience, some criteria for identification of the fistula may be suggested when clinical suspicion is raised.

Anatomical assessment

Assessment of unilateral as well as multilateral fistulous vessels originating from one or more coronary arteries, entering into the outflow site, identification of the fistulous jet within the entry site, and demonstration of the presence or absence of a dilated donor artery. Dilatation of the fistula-related artery is thought to be present when a disproportionate relation is found between the size of the coronary artery and the amount of myocardial territory it supplies.

Physiological assessment

Signal loss (flow void), which is detected when an influxing jet of turbulent flow into 2 perpendicular planes (e.g., transversal and sagittal), is seen waxing and waning into the recipient cardiac chambers or great thoracic vessels. Patients suitable for CMR application are those with symptomatic congenital CAFs originating from the right, left or both coronary arteries and terminating into the right half of the heart.

CONCLUSION

CMR is a non-invasive method that may provide additional anatomic information and shunt flow measurement as compared to conventional CAG in CAFs, provided that the diameter of the fistulous vessel is large enough. Further improvement of CMR techniques and future study of a larger number of cases are needed for more precise assessment.

CMR is useful not only for identification of CAFs but also for delineating their sites of origin and drainage. Furthermore, CMR may provide, in some CAFs patients, additional physiological data and definitive confirmation of CAFs. With its current performance, however, it is not the diagnostic modality of first choice when this anomaly is suspected and a prospective study with high resolution 3D CMR imaging is warranted.

Study limitations

The present study included a small sample of patients. In spite of this limited number of patients, a good correlation was found between the CMR measured and CAG assessed diameter of the fistulous vessels

In this single-blind retrospective study, we investigated the capability of CMR to detect the angiographically proven CAFs. The small sample size and the design of the study did not permit the calculation of the sensitivity and specificity of CMR for a given size CAFs. Only in patients where CAG and CMR were available, a comparison could be made. It comprised a small number of survey-based subjects. In view of the limited number of patients studied for flow measurement by CMR, the comparison was limited between the two methods. Future prospective studies in large number of patients with continuous murmur are required to determine the clinical value of CMR in patients with CAFs.

The authors appreciate the assistance of Dutch Cardiac Centres (appendix 1) and of Mrs. M.A. Belderok and Mr. M. Mintjens during the preparation of the manuscript.

REFERENCES

1. Wertheimer JH, Toto A, Goldman A, et al. Magnetic resonance imaging and two-dimensional and Doppler echocardiography in the diagnosis of coronary cameral fistula. *Am Heart J* 1987;114:159-62.
2. Velvis H, Schmidt KG, Silverman NH, et al. Diagnosis of coronary artery fistula by two-dimensional echocardiography, pulsed Doppler ultrasound and color flow imaging. *J Am Coll Cardiol* 1989;14:968-76.
3. Said S. Doppler echocardiographic findings in coronary-pulmonary fistula. *Int J Cardiol* 1989;25:343-6.
4. Kubota S, Suzuki T, Murata K. Cine magnetic resonance imaging for diagnosis of right coronary-arterial ventricular fistula. *Chest* 1991;100:735-7.
5. Said SAM, Vriesendorp WJS, van der Werf T. Een man met febris intermittens, algehele malaise en diastolisch hartgeruis (in Dutch). *Hartbulletin* 1998;29:206-9.
6. Umaña E, Massey CV, Painter JA. Myocardial ischemia secondary to a large coronary-pulmonary fistula. A case report. *Angiology* 2002;53:353-7.
7. Szolar DH, Sakuma H, Higgins CB. Cardiovascular application of magnetic resonance flow and velocity measurements. *J Magn Reson Imaging* 1996;6:78-89.
8. Vandenbossche JL, Felice H, Grivegne A, et al. Noninvasive imaging of left coronary arteriovenous fistula. *Chest* 1988;93:885-7.
9. Sato Y, Ishikawa K, Sakurai I, et al. Magnetic resonance imaging in diagnosis of right coronary arteriovenous fistula: a case report. *Jpn Circ J* 1997;61:1043-6.
10. Duerinckx AJ, Shaaban A, Lewis A, et al. 3D MR imaging of coronary arteriovenous fistulas. *Eur Radiol* 2000;10:1459-63.

11. Heyne J, Leder U, Pohl P, et al. Imaging of a coronary vessel anomaly with aneurysm and arteriovenous fistula by means of MR bolustracking technique. *Radiologe* 2001;41:506–10.
12. Parga JR, Ikari NM, Bustamante LNP, et al. MRI evaluation of congenital coronary artery fistulae. *Brit J Radiol* 2004;77:508–11.
13. Levin DC, Fellows KE, Abrams HL. Hemodynamically significant primary anomalies of the coronary arteries: angiographic aspects. *Circ* 1978;58:25–34.
14. Schumacher G, Roithmaier A, Lorenz HP, et al. Congenital coronary artery fistula in infancy and childhood: diagnostic and therapeutic aspects. *Thorac Cardiovasc Surg* 1997;45:287–94.
15. Said SAM, van der Werf T. Dutch survey of coronary artery fistulas in adults: Congenital solitary fistulas. *Int J Cardiol* 2006;106:323–32.
16. Said SAM, van der Werf T. Dutch survey of coronary artery fistulas in adults: Congenital coronary artery-left ventricular multiple micro-fistulas. *Int J Cardiol* 2006;110:33–9.
17. Aintablian A, Hamby RI, Hoffman I, et al. Coronary ectasia: Incidence and results of coronary bypass surgery. *Am Heart J* 1978;96:309–15.
18. Deshpande VS, Shea SM, Chung YC, et al. Breath-hold three-dimensional true-FISP imaging of coronary arteries using asymmetric sampling. *J Magn Reson Imaging* 2002;15:473–8.
19. Keegan J, Gatehouse PD, John AS, et al. Breath-hold signal loss sequence for the qualitative assessment of blood flow disturbances in cardiovascular MR. *Proc Intl Soc Mag Reson Med* 2002;10:1721.
20. Bland JM, Altman DG. Statistical methods for assessing agreement between two methods of clinical measurement. *Lancet* 1986;1:307–10.
21. Hsieh KS, Huang TC, Lee CL. Coronary artery fistulas in neonates, infants, and children: clinical findings and outcome. *Pediatr Cardiol* 2002;23:415–9.
22. Taoka Y, Nomura M, Harada M, et al. Coronary-pulmonary artery depicted by multiplanar reconstruction using magnetic resonance imaging. *Jpn Circ J* 1998;62:455–7.
23. Post JC, van Rossum AC, Hofman MB, et al. Protocol for two-dimensional magnetic resonance coronary angiography studied in three-dimensional magnetic resonance data sets. *Am Heart J* 1995;130:167–73.

APPENDIX 1

Participating Dutch centres (in alphabetical order)

W.G. de Voogt, MD, R.G.E.J. Groutars, MD, B. Ilmer, MD, A.R. Willems, MD, J. Visser, MD, St Lucas-Andreas Hospital Amsterdam; W.A.A.J. van Ekelten, MD, P.E. Polak, MD, St Anna Hospital Geldrop; J.A.J. de Boo, MD, A.H. Liem, MD, H.W.O. Roeters van Lennep, MD, Oosterschelde Hospital Goes; B. van Vlies, MD, A.J. Funke Küpper, MD, Kennemer Gasthuis Haarlem; A. Derks, MD, H.T. Droste, MD, J.H. Fast, MD, Hospital group Twente, Location Hengelo; D.G. de Waal, MD, Waterland Hospital Purmerend; D.E.P. de Waard, MD, Antonius Hospital Sneek; C.L.J.M. van Engelen, MD, Zaans Medical Centre De Heel Zaandam; W.J. Louridtz, MD, H.A. Oude Luttikhuis, MD, Isala clinics, location Sophia, Zwolle.